

Cost-effective laser interference lithography using a 405 nm AlInGaN semiconductor laser

Ikjoo Byun and Joonwon Kim

Department of Mechanical Engineering, Pohang University of Science and Technology, San 31, Pohang, Gyungbuk 790-784, Korea

E-mail: pupoi@postech.ac.kr and joonwon@postech.ac.kr

Received 9 February 2010, in final form 12 March 2010

Published 23 April 2010

Online at stacks.iop.org/JMM/20/055024

Abstract

This paper presents a cost-effective interference lithography system that uses a 405 nm AlInGaN semiconductor laser. This method is cost-effective because the AlInGaN semiconductor laser has a long coherence length (~ 20 m) and low price (e.g. only 1/3 that of the HeCd laser). This system successfully fabricated uniform nano-periodic patterns (line, dot and hole) in a photoresist (PR) over a 2×2 cm sample area. The PR patterns agreed well with simulations. Tall silicon nano-structures were fabricated by deep reactive ion etching (DRIE) using a PR pattern as a direct etch mask layer. Aspect ratios of 25 with smooth and vertical sidewalls were achieved after 32 DRIE cycles.

(Some figures in this article are in colour only in the electronic version)

1. Introduction

Interference lithography (IL) is an effective method of fabricating nano-periodic patterns over a large area [1]. In the most common form of IL, two or more mutually coherent light waves interfere to form a sinusoidal intensity distribution, which is recorded on a photosensitive material. IL has two advantages over other lithography methods: (1) it does not require a photomask, so patterns with various sizes and shapes can be fabricated easily by changing the configuration of the system, and (2) its resolution is limited only by the wavelength used. Although IL has the limitation that it can only fabricate simple periodic patterns, it is an attractive alternative to conventional methods for applications in which periodic patterns are desirable, including x-ray transmission gratings [2], photonic crystals [3] and sub-micrometric sieves [4].

To obtain a large exposure area, IL requires a laser with a long coherence length L_C (i.e. a few tens of centimeters) [5]. A commercially available HeCd laser offers an L_C of 30 cm, so it allows IL to be applied over a 2×2 cm area [5, 6]. The L_C of Ar-ion lasers is long enough to fabricate patterns over a 100 mm diameter wafer [7], and a Kr-ion laser has been used to fabricate a uniform photoresist (PR) post on a 50 \times

50 cm glass substrate [8]. However, Ar-ion and Kr-ion lasers are too expensive (usually > US\$ 50 000) for most laboratories. Therefore, although IL has many advantages for fabricating nano-periodic patterns, its applicability is limited by the cost of the laser. Recently, use of an inexpensive 405 nm diode laser as a source for IL has been reported, but the patterning area was small (~ 1 mm²) due to its insufficient coherence length [9].

This paper introduces a cost-effective IL system that uses a 405 nm AlInGaN semiconductor laser for a large exposure area. This system was used to fabricate well-defined nano-periodic line arrays, dot arrays and post arrays with periods from 290 nm to 750 nm over a 2×2 cm area. The shapes of these patterns agreed well with simulation results. Notably, the cost of the apparatus was <US\$ 15 000 including the laser source.

2. System design

2.1. Lloyd's mirror interferometer

This experiment applied a Lloyd's mirror interferometer, which consists of a mirror fixed perpendicularly to the

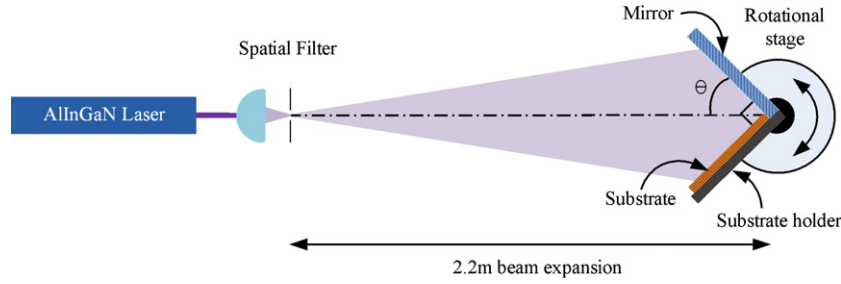


Figure 1. Schematic of Lloyd's mirror interferometer for interference lithography.

specimen (figure 1). In Lloyd's interferometer the period P of an interference pattern is given by

$$P = \frac{\lambda}{2 \sin \theta}, \quad (1)$$

where λ is the laser wavelength and θ is the incident angle to the specimen. Two beams are used: one travels directly to the specimen and the other is reflected onto the specimen by a mirror. These two beams form an interference pattern on the specimen.

2.2. Fabricating a uniform pattern by Lloyd's mirror interferometer

For IL to fabricate a uniform pattern, the visibility V and the linewidth uniformity U should be considered. V is defined as

$$V = \frac{D_{\text{MAX}} - D_{\text{MIN}}}{D_{\text{MAX}} + D_{\text{MIN}}}, \quad (2)$$

where D_{MAX} and D_{MIN} are the maximum and minimum values of the sinusoidal dose distribution, respectively [10]. V can have values between 0 and 1, with 0 being equal to a flood exposure and 1 being ideal interference. U of an interference pattern is affected by the exposure dose [5]; for patterns with the same period, a 30% change in the exposure dose can cause an $\sim 10\%$ change in U [11]. Therefore, to obtain a high-quality interference pattern with good U over the exposure area, V must be close to 1 and the variation of the exposure dose should be minimized over the exposure area.

2.2.1. Visibility in Lloyd's mirror interferometer. The configuration of Lloyd's mirror interferometer causes the beams from the laser to travel different distances (i.e. the optical path difference, OPD) to the specimen (figure 2). This OPD reduces the mutual coherence of interfering beams, which, in turn, reduces the V because the source has a limited coherence length. V can also be rewritten as a function of OPD and the L_C of the source (3) [12]:

$$V = \exp \left[- \left(\frac{\pi \times \text{OPD}}{2L_C} \right)^2 \right]. \quad (3)$$

V decreases as OPD increases, at a rate that diminishes as L_C increases (figure 3). L_C of 20 m can be estimated to induce V close to 1 over several tens of centimeters of OPD.

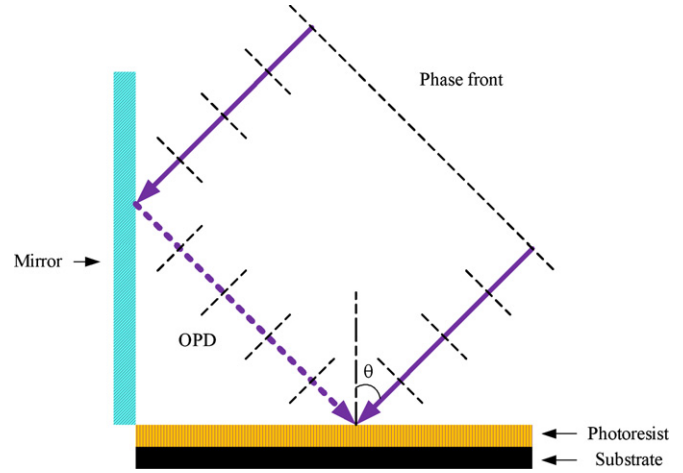


Figure 2. Optical path difference (OPD) in Lloyd's mirror interferometer.

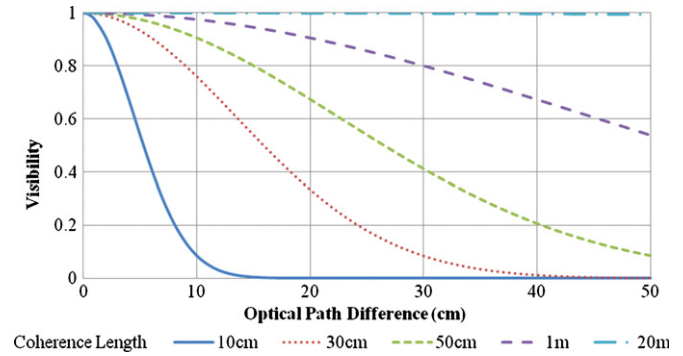


Figure 3. V as a function of OPD and L_C .

2.2.2. Gaussian intensity distribution in Lloyd's mirror interferometer. The intensity profile of a laser beam induces the difference of the exposure dose over the exposure area at the same exposure time, and it reduces U . The intensity I of a laser beam can be assumed to diminish radially following a Gaussian distribution centered on the spatial filter:

$$I = I_0 \exp \left(\frac{-2r^2}{\omega_0^2} \right), \quad (4)$$

where ω_0 is the Gaussian beam radius, r is the distance from the center of beam and I_0 is the peak intensity

$$I_0 = \frac{2P_S}{\pi \omega_0^2}, \quad (5)$$

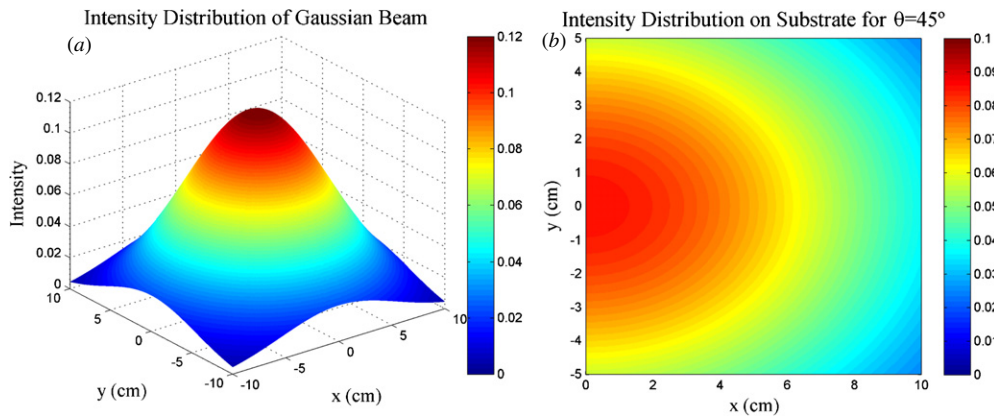


Figure 4. Simulation of intensity distribution: (a) intensity distribution of the Gaussian beam at $\omega_0 = 11$ cm and (b) intensity distribution on the substrate at $\omega_0 = 11$ cm and $\theta = 45^\circ$.

where P_S is the total source power (figure 4(a)). For good U over the exposure area, the size of the specimen is limited by the size of the areas over which intensity distribution is uniform. When $\theta = 45^\circ$, the intensity difference over a 2×2 cm area from the origin is 5%, so the pattern in this area may have a good U (figure 4(b)).

2.3. Laser source and optical components

A 30 mW AlInGaN semiconductor laser at $\lambda = 405$ nm in single longitudinal mode (BCL-030-405-S, CrystaLaser) was chosen for the source. It offers a very long L_C (~ 20 m) which provides the maximum V in our setup. It is cheaper than other HeCd, Ar-ion or Kr-ion lasers, does not need any cooling fans and has a short warm-up period. It is also small, so it is easy to handle. Thus, this laser is potentially a good IL tool.

In our experiment, a transverse electric mode polarized laser beam was focused by an aspherized achromatic lens (focus length = 14 mm) onto a pinhole (diameter = $10 \mu\text{m}$) and spatially filtered while passing through the pinhole. The beam had a diameter of 22 cm when it reached the exposure stage. An enhanced aluminum mirror (reflectance $> 95\%$ at $\lambda = 405$ nm) was used to obtain a high-contrast interference pattern.

3. Methods

A single-crystal (1 0 0) silicon substrate was cleaned with a mixture of H_2SO_4 and H_2O_2 (4:1 v:v), immersed in buffered oxide etchant for several seconds to remove native SiO_2 , and then dehydrated on a hot plate for 10 min at 150°C . As an adhesion promoter, a mixture of propylene glycol monomethyl ether acetate (PGMEA) and hexamethyl disilazane (4:1 v:v) was applied to the substrate by spin-coating at 5000 rpm for 35 s. Then a mixture of positive PR (AZ5214-E, Clariant) and PGMEA (1:2 v:v) was spin-coated on the substrate at 5000 rpm for 35 s to form a PR layer ~ 200 nm thick. After spin coating, the substrate with PR was soft-baked at 95°C for 20 s on a hot plate. This baking time was chosen on the basis of preliminary trials (data not presented). After soft baking, the substrate was exposed under the IL setup with

the appropriate exposure dose. The maximum exposure dose was 36 mJ for line patterning ($P = 290$ nm), and the minimum exposure dose was 21.6 mJ for hole patterning ($P = 750$ nm).

For fabricating a two-dimensional dot or hole pattern, a double exposure technique was applied. This technique involves a first exposure, and then a second exposure after rotating the substrate holder. After the exposure step, the substrate was developed by immersion in 0.255 N, tetramethyl ammonium hydroxide-based developer (AZ500MIF, Clariant), at room temperature (25°C) with no agitation. After development, the substrate was rinsed with de-ionized water and blow-dried using N_2 gas. The residual PR layer was removed using O_2 plasma at 600 W with 25 sccm of O_2 for 5 s using a multiplex ASE-SR ICP (STS). The PR pattern was transferred to the silicon substrate using deep reactive ion etching (DRIE) using the multiplex ASE-SR ICP. The remaining PR was removed using O_2 plasma. After processing, the sample was inspected by field-emission scanning electron microscopy (FE-SEM, JEOL JMS-7400F, operating at 2 keV).

4. Results and discussion

4.1. PR nano-patterns by IL

To fabricate a pattern with a smaller distance between features (period), θ should be increased. Increasing θ spreads the beam energy over a larger area of the exposure plane and increases the fraction of the reflected beam on the PR surface. Therefore, the exposure time must be increased if the exposure dose is to be held constant.

IL was used to obtain one-dimensional PR line patterns with periods of 290 nm (figure 5(a)) and 750 nm (figure 5(b)). Different exposure times were used to obtain these patterns. IL was also used to obtain two-dimensional PR patterns with different shapes using the double exposure technique (figure 6); as the exposure dose increased, the patterns changed from holes (figure 6(a)) to squares (figure 6(b)) to posts (figure 6(c)).

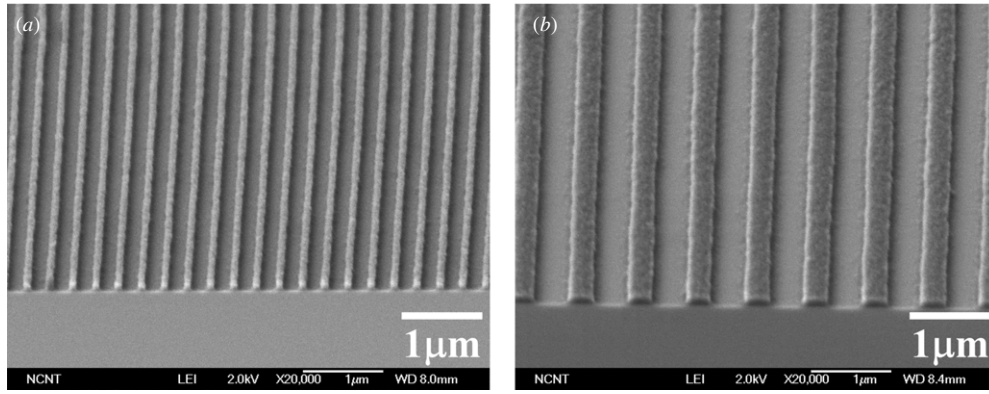


Figure 5. SEM images of the 1D PR line pattern: (a) $P = 290$ nm, exposure time = 300 s and (b) $P = 750$ nm, exposure time = 190 s.

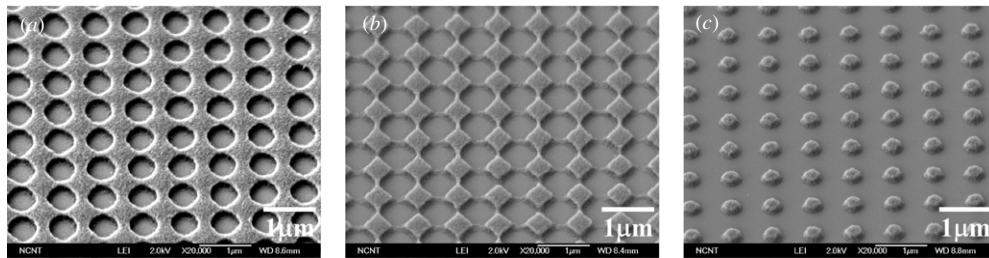


Figure 6. SEM images of the 2D PR pattern varying the exposure time only ($P = 750$ nm). Substrates were irradiated twice. Exposure times: (a) 90 s + 90 s, (b) 120 s + 120 s and (c) 135 s + 135 s.

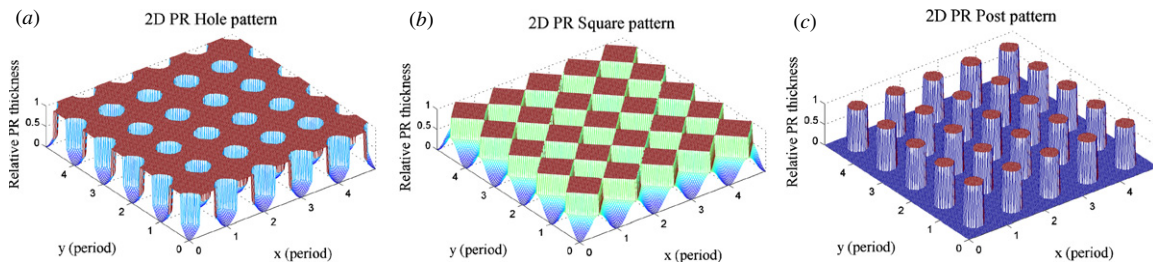


Figure 7. Simulation results of the 2D PR pattern: (a) hole, (b) square and (c) post.

4.2. Simulation of a pattern profile

Parts of the PR layer are developed only if they are illuminated with more than a threshold energy, which can be represented as a plane in the sinusoidal interference profile. Thus, the expected PR profile corresponds to the locations at which intensities are greater than this plane. The expected profile of the interference beam and the resulting PR pattern fabricated by IL were simulated using MATLAB (The MathWorks) for a pattern profile that consists of an array of squares. The shape of the simulated pattern changed from hole to post as the exposure dose increased (figure 7); these results agree well with the experimental results (figure 6).

4.3. Fabrication of silicon nano-structures with a smooth and vertical sidewall by deep reactive ion etching (DRIE)

DRIE was employed to transfer the PR nano-pattern into a silicon substrate for tall structures (i.e. $>1 \mu\text{m}$). DRIE has rarely been used to construct nano-structures because the

Table 1. Process parameters in DRIE to obtain tall silicon structures with smooth and vertical sidewalls.

Cyclic step	Etching	Passivation
Gas flow rate (sccm)	SF ₆ : 50, O ₂ : 5	C ₄ F ₈ : 80
Active time (s)	3	2
Coil RF power (W)	350	350
Platen RF power (W)	15	0

sidewall rippling (scalloping) is a serious problem on the nano-scale [6]. To obtain tall structures with smooth and vertical sidewalls, the process parameters in DRIE were changed (table 1) compared with the standard values.

Silicon nano-structures with different periods and shapes were etched by DRIE using the PR pattern as a direct etch mask layer. Smooth and vertical sidewalls were obtained (figure 8). The height of structures was constant at the same cyclic steps regardless of the size and shape of the PR pattern. High-aspect-ratio (i.e. 25) nano-structures were achieved after 32 DRIE

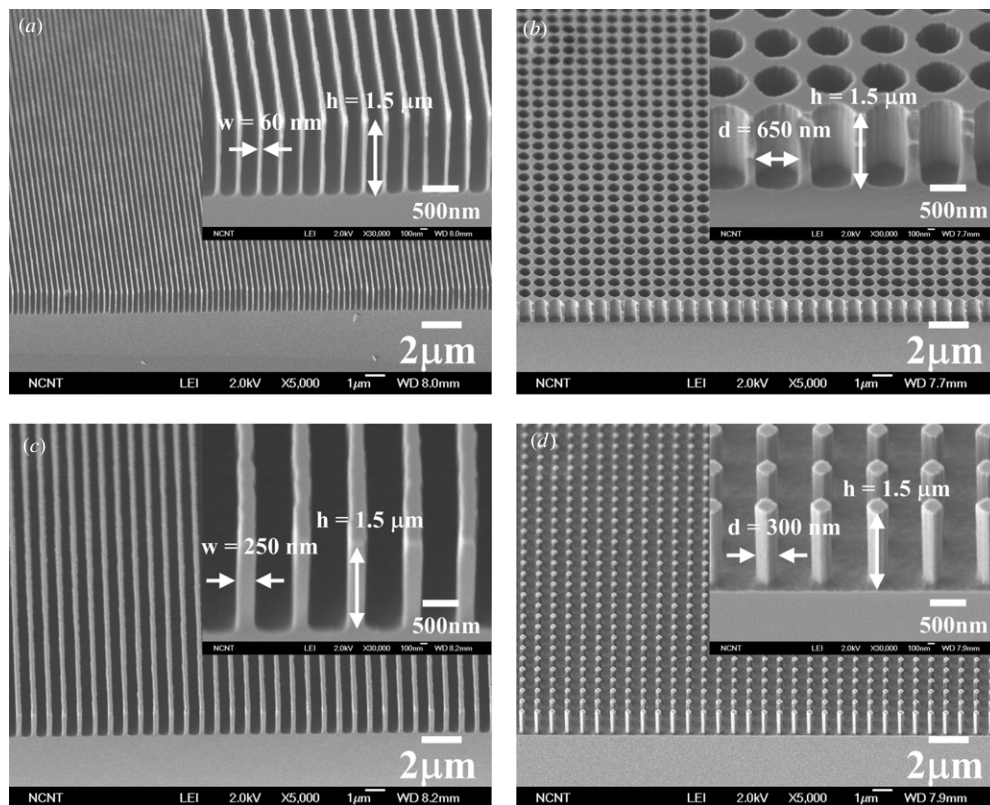


Figure 8. SEM images of Si nano-structures fabricated by interference lithography after 32 cyclic steps of DRIE: (a) line pattern, $P = 290$ nm; (b) hole pattern, $P = 750$ nm; (c) line pattern, $P = 750$ nm and (d) post pattern, $P = 750$ nm.

cycles (figure 8(a)); the etching depth could be increased by using more cycles.

5. Conclusion

We have demonstrated a cost-effective method for IL fabrication of nano-periodic structures over a large sample area using an AlInGaN semiconductor laser. This laser has a longer L_C (~ 20 m) and a lower cost than the HeCd laser which is commonly used for IL. Our IL system can be installed at a cost < US\$ 15 000, and so meets the demand for an economical IL system. Moreover, compared to the HeCd laser, our system has a longer L_C and a greater exposure area, and so can fabricate high-quality patterns over a larger area.

The period of pattern was easily changed from 290 nm to 750 nm by rotating the substrate holder. Using the double exposure technique, two-dimensional hole, square and dot patterns were fabricated by controlling the exposure dose. The patterns agreed well with simulation results. The PR nano-patterns were transferred to a silicon substrate using DRIE. The transferred patterns had smooth and vertical sidewalls, and structures with high aspect ratios (i.e. 25) were obtained by 32 cyclic steps of DRIE. We expect that even higher aspect ratios can be obtained using more DRIE cycles. Due to the cost-effectiveness, this method of fabricating nano-periodic structures is expected to be applied easily in many industries and fields of research.

Acknowledgments

This work was supported by a grant to the MEMS Research Center for National Defense funded by the Defense Acquisition Program Administration and the Nuclear Research and Development Program of the National Research Foundation of Korea (NRF) funded by the Ministry of Education, Science and Technology (MEST) (grant code: MZ0706000050-08M0600-05010).

References

- [1] Solak H H 2006 Nanolithography with coherent extreme ultraviolet light *J. Phys. D: Appl. Phys.* **39** R171–88
- [2] Schattenburg M L, Canizares C R, Dewey D, Flanagan K A, Hamnett M A, Levine A M, Lum K S K, Manikkalingam R, Markert T H and Smith H I 1991 Transmission grating spectroscopy and the advanced x-ray astrophysics facility *Opt. Eng.* **30** 1590–600
- [3] Campbell M, Sharp D N, Harrison M T, Denning R G and Turberfield A J 2000 Fabrication of photonic crystals for the visible spectrum by holographic lithography *Nature* **404** 53–6
- [4] Gurierrez-Rivera L E and Cescato L 2008 SU-8 submicrometric sieves recorded by UV interference lithography *J. Micromech. Microeng.* **18** 115003
- [5] O'Reilly T B and Smith H I 2008 Linewidth uniformity in Lloyd's mirror interference lithography systems *J. Vac. Technol. B* **26** 2131–4
- [6] Choi C-H and Kim C-J 2006 Fabrication of a dense array of tall nanostructures over a large sample area with sidewall

- profile and tip sharpness control *Nanotechnology* **17** 5326–33
- [7] Schattenburg M L, Aucoin R J and Fleming R C 1995 Optically matched trilevel resist process for nanostructure fabrication *J. Vac. Sci. Technol. B* **13** 3007–11
- [8] Spallas J P, Boyd R D, Britten J A, Fernandez A, Hawryluk A M, Perry M D and Kania D R 1996 Fabrication of sub-0.5 mm diameter cobalt dots on silicon substrates and photoresist pedestals on 50 cm × 50 cm glass substrates using laser interference lithography *J. Vac. Sci. Technol. B* **14** 2005–7
- [9] Fucetola C P, Korre H and Berggren K K 2009 Low-cost interference lithography *J. Vac. Sci. Technol. B* **27** 2958–61
- [10] O'Reilly T B and Smith H I 2008 Photoresist characterization using double exposure with interference lithography *J. Vac. Sci. Technol. B* **26** 128–31
- [11] Agayan R R, Banyai W C and Fernandez A 1998 Scaling behavior in interference lithography *Proc. SPIE* **3331** 662–72
- [12] Walsh M E 2004 On the design of lithographic interferometers and their application *PhD Thesis* Massachusetts Institute of Technology